Editors Suggestion

Heterogeneous Activation, Local Structure, and Softness in Supercooled Colloidal Liquids

Xiaoguang Ma,[1,2,*] Zoey S. Davidson,[1] Tim Still,[1] Robert J. S. Ivancic,[1]
S. S. Schoenholz,[3] A. J. Liu,[1] and A. G. Yodh[1]
[1]Department of Physics & Astronomy, University of Pennsylvania, Philadelphia, Pennsylvania 19104, USA
[2]Complex Assemblies of Soft Matter, CNRS-Solvay-UPenn UMI 3254, Bristol, Pennsylvania 19007-3624, USA
[3]Google Brain, 1600 Amphitheatre Parkway, Mountain View, California 94043, USA

(Received 4 February 2018; revised manuscript received 8 August 2018; published 18 January 2019)

We experimentally characterize heterogeneous nonexponential relaxation in bidisperse supercooled colloidal liquids utilizing a recent concept called "softness" [Phys. Rev. Lett. **114**, 108001 (2015)]. Particle trajectory and structure data enable classification of particles into subgroups with different local environments and propensities to hop. We determine residence times t_R between particle hops and show that t_R derived from particles in the same softness subgroup are exponentially distributed. Using the mean residence time $\bar{t}_R$ for each softness subgroup, and a Kramers' reaction rate model, we estimate the activation energy barriers E_b for particle hops, and show that both $\bar{t}_R$ and E_b are monotonic functions of softness. Finally, we derive information about the combinations of large and small particle neighbors that determine particle softness, and we explicitly show that multiple exponential relaxation channels in the supercooled liquid give rise to its nonexponential behavior.

DOI: 10.1103/PhysRevLett.122.028001

When a liquid is cooled rapidly past a characteristic onset temperature, its dynamics become increasingly slow, nonexponential, and inhomogeneous [1–5]; this is the glass transition. In crystalline systems, successful theories of dynamics have been developed based on structural topological defects. The prospect of an analogous approach to glassy dynamics, premised on structural heterogeneities, is therefore appealing. For many years, however, no structural order parameter predictive of dynamics was identified, and until recently, it has remained unclear whether a connection between structure and dynamics exists at all [6–16].

Very recent studies have shown that data from molecular dynamics simulations or experiments can be analyzed with machine learning methods to infer a structural order parameter for dynamics in supercooled liquids and disordered solids called "softness" [17–23]. An analysis based on softness was applied to supercooled liquids, and was shown to simplify conceptual understanding of phenomena such as heterogeneous dynamics and nonexponential relaxation [18], history dependence during aging [19], and dynamics in thin films [20]. Additionally, softness correlations were shown to correlate with the size of rearrangements in simulations and experiments on supercooled liquids [22]. Despite these successes, the testing of the conceptual utility of softness has been limited to date to *simulations*. Besides imaging and statistical challenges, the chief hurdle in applying the analysis to experiments is that the approach has required data taken at many different temperatures to infer the many Arrhenius relaxation processes that coexist in the system.

In this Letter we apply the softness concept to experimental supercooled liquids. We corroborate the results in Ref. [18] and show directly that structure-dependent energy barriers may be ascertained from a thermal supercooled colloidal liquid at a *single* temperature. We then leverage the heterogeneous distribution of energy barriers to demonstrate that it explains nonexponential relaxation observed in the sample [24–27]. To avoid taking data at multiple temperatures, we determine the residence times between successive rearrangements of individual particles and show that the residence time distribution, conditioned on softness, is exponential with a timescale that is monotonic in the softness; multiple thermal activations characterized by the same decay time are associated with particles of same softness. We use the measured individual exponential residence times to derive the distribution of residence times of the entire system; this calculated system distribution is nonexponential and agrees well with experiment. Therefore, relaxation in our supercooled colloidal liquid is *not* intrinsically nonexponential [26,27]. Together, the measurements of relaxation time, softness, and energy-basin shape from particle trajectories in a single sample at fixed temperature and density, along with a Kramers reaction rate model [28–31], enable us to derive a distribution of effective free energy activation barriers in the supercooled colloidal liquid.

Finally, we investigate the connection between softness and local structure. We show that in bidisperse colloidal supercooled liquids, softer particles tend to have fewer nearby large particles. Our results demonstrate a direct connection between the local structural environment of a

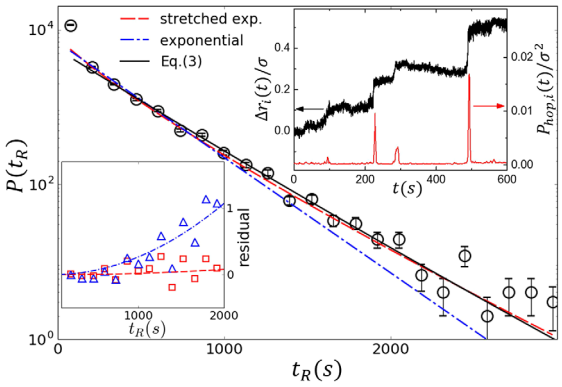

FIG. 1. $P(t_R)$ measured for large particles. Error bars indicate standard deviations. The red dashed line is the stretched exponential fit $P(t_R) \sim \exp[-(t_R/220)^{0.85}$. The black solid line is calculated from Eq. (3). The blue dash-dot line is the exponential fit $P(t_R) \sim \exp[-(t_R/300)]$. Inset (left): the relative residuals of both fits. The residual plot is cut off at 2000 sec; points at longer times exhibit even greater disagreement with the exponential fit, but obscure early-time data which have excellent signal-to-noise. Residuals are fit with quadratic functions as guides for the eye. Inset (right) shows a trajectory (black) of particle displacement, $\Delta r_i(t) \equiv |r_i(t) - r_i(0)|$, relative to an arbitrary reference time $t = 0$. Here, displacement is scaled by large particle diameter, σ. $p_{\mathrm{hop},i}$ is calculated from the same trajectory.

particle, its dynamics, and the energy barriers it must overcome to rearrange. The experiments show explicitly that the combination of exponential processes that leads to nonexponential relaxation in our glassy colloidal liquid has its origin in structural heterogeneity at the particle scale.

We study aqueous experimental samples (see Supplemental Material [32]) composed of a monolayer of poly(N-isopropylacrylamide) (PNIPAM) hydrogel microspheres [33] sandwiched between two cover glasses. Observations are carried out by bright-field video microscopy (Leica DMR) with a $100\times$ oil-immersion lens. The video is recorded by a CCD camera (UNIQ 900DS) at 10 frames per second with a resolution of 1392×1036 and 256 gray scale. We utilize Trackpy [34,35] to track particle trajectories. The sample temperature is maintained at 28 °C by an objective heater (BiOptechs). The viewing area contains $N_l \simeq 3800$ large and $N_s \simeq 4200$ small particles [l (s) represents large (small) particles]. The diameters, $\sigma = 1.2$ and $\sigma' = 0.9$ μm, of the large and small species, respectively, are obtained from the first peaks of the radial distribution functions, $g_l^l(r)$ and $g_s^s(r)$. The packing fraction $\pi[N_l(\sigma/2)^2 + N_s(\sigma'/2)^2]/A$ (A is the area of field) is calculated to be 0.84.

Particle displacement trajectories are characterized by many intermittent jumps, rather than the more continuous random walks found in liquids. A typical displacement, $\Delta r_i(t) \equiv |r_i(t) - r_i(0)|$, of the ith particle is shown in Fig. 1, right inset. This motion exhibits idle periods separated by short-time hoplike relocations. To quantify these intermittent dynamics, we compute the particle "hop" function [18,36,37], $p_{\mathrm{hop},i}(t) = [\langle (r_i - \langle r_i \rangle_B)^2 \rangle_A \langle (r_i - \langle r_i \rangle_A)^2 \rangle_B]^{1/2}$; here the angular brackets $\langle \ldots \rangle_A$ and $\langle \ldots \rangle_B$ denote an average over the time windows $A \equiv [t - \delta t/2, t$ and $B \equiv [t, t + \delta t/2$, respectively. We choose the hop duration parameter $\delta t = 8s$ (Supplemental Material [32]). Notice, $p_{\mathrm{hop},i}(t)$ remains close to zero except when the particle hops to a new position; then $p_{\mathrm{hop},i}(t)$ exhibits a large peak (Fig. 1, inset).

Intermittency in particle trajectories is characterized by a residence time parameter, t_R, defined as the separation between successive $p_{\mathrm{hop},i}$ peaks. To derive t_R from the $p_{\mathrm{hop},i}$ trajectory, we choose the threshold value $p_{\mathrm{hop},c}/\sigma^2 = 0.002$ (Supplemental Material [32]) to distinguish local vibrational motion from hops. The probability distribution function (PDF), $P(t_R)$, measured from all $p_{\mathrm{hop},i}$ is shown in Fig. 1. The excess in distribution events at the shortest times ($t_R < 200$ s) is due to the crossover of large vibrational fluctuations and small hops. The longer-time distribution ($t_R > 200$ s) is well fit by the stretched exponential function, $\tilde{P}(t_R) \sim \exp[-(t_R/\tau)^{\beta}$, with $\tau = 220 \quad 37$ and $\beta = 0.85 \quad 0.04$ (see Fig. 1). Note, dynamic light scattering measurements of hydrogel-particle glass formers found similar β; smaller β were reported in more fragile hard-sphere glass formers [38]. Fitting $P(t_R)$ with exponential form [i.e., $\tilde{P}(t_R)$ with $\beta = 1$] was also tested and found to be quantitatively worse, based on residuals, $[P(t_R) - \tilde{P(t_R)}]/P(t_R)$ (Fig. 1) and chi-square errors (Supplemental Material [32]). Since hopping time statistics are directly related to dynamical correlation functions [39–41], the stretched exponential $P(t_R)$ reflects complex relaxation in the supercooled regime. Though many explanations exist for the nonexponential process [26,27], early work [24,25] and recent simulations [18–20] suggest they arise when thermal activations involve a range of energy barriers.

Incorporation of the softness concept enables use of $P(t_R)$ to understand the microscopic energy landscape in a deeper way. To this end, we follow Refs. [17,18] and describe the local structure near the ith particle using the following radial density function

$$G_i^X(\mu) = \sum_{j \neq i} \exp - \frac{R_{ij} - \mu}{0.1\sigma}^2 . \qquad (1)$$

Here, R_{ij} is the distance between particles i and j; μ is a probing radius from 0.4σ to 5.0σ in 0.1σ increments (47 μ's in total), and $X \in \{l, s\}$ denotes the species of particle j.

For the bidisperse sample, we utilize 94 $G_i^X(\mu)$ to represent the instantaneous local structure of the ith particle [a point in a 94-dimensional (94D) hyperspace]. We next identify two groups of particles with "opposite" mobilities following [18]: "soft" particles are on the verge of a hop, and "hard" particles have the longest residence times.

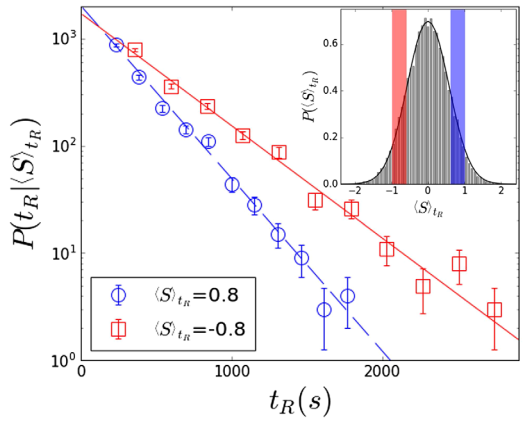

FIG. 2. Two unnormalized conditional PDFs, $P(t_R|\langle S\rangle_{t_R})$, for t_R with similar $\langle S\rangle_{t_R}$. The red solid and blue dashed lines are exponential fits, $P(t_R|\langle S\rangle_{t_R}) \sim (1/\bar{t}_R)e^{-t_R/\bar{t}_R}$, with $\bar{t}_R = 400$ and 270 sec for $\langle S\rangle_{t_R} = -0.8$ and 0.8, respectively; fitting is to the tails ($t_R > 200$ sec) of the conditional PDFs. Inset shows the overall PDF, $P(\langle S\rangle_{t_R})$. The solid line is a Gaussian fit. The subgroups that constitute the conditional PDFs are shaded with the same colors.

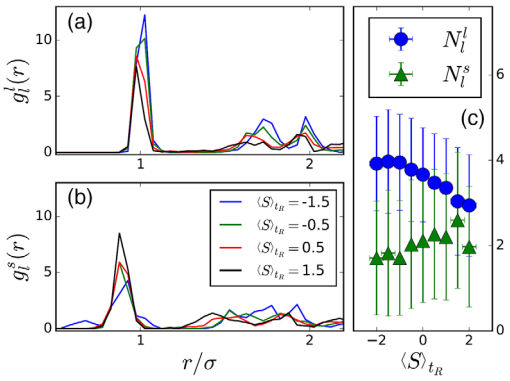

FIG. 3. (a) Measured $g_l^l(r)$ of large particles around a central large particle. (b) Measured $g_l^s(r)$ of small particles around a central large particle. (c) Numbers of large (blue circle) and small (green triangle) neighbors within $r < 1.2\sigma$ as a function of $\langle S\rangle_{t_R}$ (see main text).

Utilizing only a few hundred examples of the softest and hardest particles, we carry out a linear classification analysis by computing the hyperplane (in the 94D hyperspace) that "best" separates soft versus hard groups using the support vector machine (SVM) method [42–44]. We compute two hyperplanes, one for large central particles and one for small central particles, to avoid misclassifications due to differences in their innate mobilities. We also explored and found that inclusion of bond orientation parameters did not significantly improve the accuracy of the hyperplane.

From the trained hyperplane, we compute softness values $S_i(t)$ of particle i at time t, for every particle throughout the entire observation period. $S_i(t)$ is the normal displacement between particle's local structure (corresponding point in the 94D hyperspace) and the best hyperplane. $S_i(t)$ is centered at zero and its distribution has a Gaussian form (Fig. 9 in the Supplemental Material [32]). Note, $S_i(t)$ exhibits different spatial correlations than bond orientation parameters [45], and its correlation length is approximately one particle diameter [Fig. 8(b) in the Supplemental Material [32]]. Indeed, short-range correlations of softness appear to be a generic feature of disordered solids [22]. The mean softness $\langle S\rangle_{t_R}$ averaged during every t_R interval was also calculated; by using the mean, we remove fluctuations due to particle vibrations, which amount to a standard deviation of $\delta S = 0.2$. The distribution of $\langle S\rangle_{t_R}$ also has a Gaussian form albeit with narrower range (Fig. 2, inset).

To explicitly show the difference in local environments captured by the softness parameter, we report the local radial distribution functions during every t_R interval. First we select all intervals that have similar $\langle S\rangle_{t_R}$, for particles of species A ($A \in \{l, s\}$); the total number of intervals selected is n_A. Then we compute the local radial distribution of B particles ($B \in \{l, s\}$),

$$g_A^B(r) = \frac{1}{n_A}\sum_A \frac{n_B(r)}{2\rho_B \pi r dr}\Bigg|_{t_R}, \tag{2}$$

where $n_B(r)$ is the instantaneous number of B particles in a circular bin of radius, r, with bin width, $dr = 0.05\sigma$, centered on the A particle; $2\pi r dr$ is the bin area. ρ_B is the number density of B particles in the viewing area.

Figure 3(a) shows the measured g_l^l for four different $\langle S\rangle_{t_R}$. Note, large particles tend to form small crystalline domains (Fig. 2 in the Supplemental Material [32]). Thus the first peaks of g_l^l are delta-function-like, and their heights depend inversely on dr. Interestingly, a monotonic decrease in the magnitude of the first three peaks of g_l^l is apparent as $\langle S\rangle_{t_R}$ increases. This observation suggests that when the density of surrounding large particles increases, the central particle tends to be harder and less likely to hop. By contrast, g_l^s displays an opposite trend in the first peak [Fig. 3(b)] suggesting that a softer environment is created by increasing surrounding small particle density. Figure 3(c) shows the numbers of large (N_l^l) and small neighbors (N_l^s) within the radial distance $r = 1.2\sigma$ from the central large particle. These results suggest that one can make a particle softer in a binary system by replacing neighboring large species with small ones. Note, g_s^l, g_s^s, N_s^l, and N_s^s of small central particles exhibited similar trends (Fig. 10 in Supplemental Material [32]).

We next group the t_R intervals from the same particle species by similar $\langle S\rangle_{t_R}$ to derive the conditional PDF, $P(t_R|\langle S\rangle_{t_R})$. Interestingly, $P(t_R|\langle S\rangle_{t_R}) = (1/\bar{t}_R)e^{-t_R/\bar{t}_R}$ has an exponential form; $\bar{t}_R$ is the mean residence time averaged over the same-softness subgroup. Figure 2 shows the exponential distributions of $P(t_R|\langle S\rangle_{t_R})$ for two large particle subgroups. Their mean softness are $\langle S\rangle_{t_R} = -0.8$ 0.2 and 0.8 0.2 and corresponding mean residence times

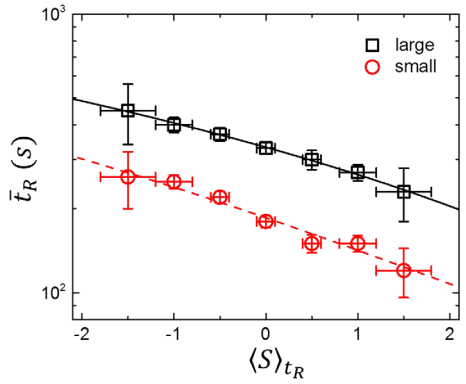

FIG. 4. (a) Measured $\bar{t}_R$ as a function of $\langle S\rangle_{t_R}$, for large (black squares) and small (red circles) particles. Solid and dashed lines are exponential fits (see main text). The error bars indicate the standard deviations.

are $\bar{t}_R = 400$ and 270 sec, respectively. A correlation between hopping rate $(1/\bar{t}_R)$ and softness was also reported in a 3D Lennard-Jones simulation [18].

The different exponential $P(t_R|\langle S\rangle_{t_R})$ provide direct experimental evidence for coexistence of multiple activation processes in the supercooled colloidal liquid. We measured $\bar{t}_R$ versus $\langle S\rangle_{t_R}$ for both species. These functions are well described (Fig. 4) by quadratic (Supplemental Material [32]) and exponential $[\bar{t}_R = \bar{t}_{R0}\exp(b\langle S\rangle_{t_R})]$ forms. Numerical fitting gives $\bar{t}_{R0} = 332$, and $b = -0.22$ for large particles, and $\bar{t}_{R0} = 186$, and $b = -0.26$ for small ones. The prefactor $\bar{t}_{R0}$ is the $\bar{t}_R$ at zero softness $\langle S\rangle_{t_R} = 0$.

Using the measured $P(t_R|\langle S\rangle_{t_R})$, and $P(\langle S\rangle_{t_R})$, we can readily compute the unnormalized $P(t_R)$ for the entire supercooled liquid sample, as a superposition of different relaxation channels distinguished by $\langle S\rangle_{t_R}$:

$$P(t_R) \equiv HW \int_{-\infty}^{\infty} d\langle S\rangle_{t_R} P(\langle S\rangle_{t_R}) P(t_R|\langle S\rangle_{t_R}). \quad (3)$$

Here H is the total number of t_Rs, and W is the bin width of $P(t_R)$. The calculated $P(t_R)$ accurately reproduces measurements (black line, Fig. 1), thereby experimentally demonstrating the origin of nonexponential relaxation in supercooled liquids with single particle resolution [14–16,26]. In addition, data from a sample at higher packing fraction (Supplemental Material [32]) confirmed that $P(t_R)$ is more stretched in more strongly supercooled samples and that the decomposition into exponential channels is still valid.

Finally, we estimate the activation energy barriers and distribution using measurements and a Kramers' reaction rate model [31,46]. Here the activation energy can be understood as the dynamic free energy due to direct interactions and entropy from neighboring particles [47–49]. The inset in Fig. 5(a) schematically shows the dynamic free energy $U(x)$, where x_0 and x_b are the metastable and transition states along the reaction coordinate x, respectively. The barrier height is defined as

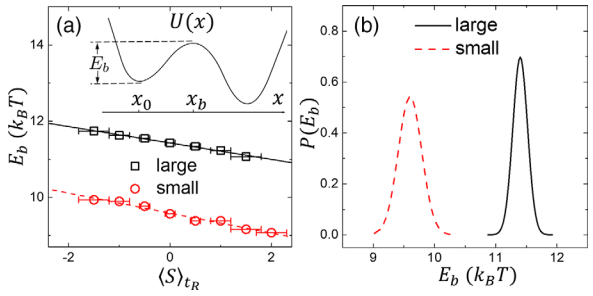

FIG. 5. (a) Estimated E_b as a function of $\langle S\rangle_{t_R}$ for both species. Inset: Schematic of the barrier-crossing activation process. (b) $P(E_b)$ of activation energy barriers.

$E_b \equiv U(x_b) - U(x_0)$. In the limit $E_b/k_BT \gg 1$, E_b is related to the mean residence time $\bar{t}_R$ by

$$\bar{t}_R \simeq \frac{2\pi k_B T}{D_{\rm sh}\sqrt{U_0''|U_b''|}} \exp\left(\frac{E_b}{k_BT}\right), \quad (4)$$

where $D_{\rm sh}$ is the short-time particle diffusion coefficient, $U_0'' \equiv [d^2U(x)/dx^2]|_{x=x_0}$ and $U_b'' \equiv [d^2U(x)/dx^2]|_{x=x_b}$ are the second derivatives of $U(x)$ at $x = x_0$ and $x = x_b$, respectively. This equation has been shown to be accurate in colloid experiments when $E_b \geq 6k_BT$ [50,51].

To use Eq. (4), one also needs $D_{\rm sh}$, U_0'', and U_b''. For large particles, we measured $D_{\rm sh} \simeq 0.04\ \mu{\rm m}^2\,{\rm s}^{-1}$ at 0.1 ms, which is one-quarter of its measured bare diffusivity $D_0 \simeq 0.16\ \mu\,{\rm m}^2\,{\rm s}^{-1}$. For small particles, D_0 was measured, and the same ratio $D_{\rm sh}/D_0$ assumed. To determine the potential curvature, we assume the distribution of particle position during a t_R follows the Boltzmann distribution, $P(x - x_0) = \exp[U(x_0) - U(x)/k_BT$, and we approximate $U(x)$ around x_0 to be harmonic, $U(x - x_0) = \frac{1}{2}U_0''(x - x_0)^2$ (Figs. 14, 15 in Supplemental Material [32]). $U_0'' = 3.2 \quad 1.0 \times 10^{-5}$ and $1.5 \quad 0.5 \times 10^{-5}\ {\rm N\,m^{-1}}$, for large and small particles, respectively. We did not measure U_b'', due to statistics. Fortunately, E_b is rather insensitive to U_b''; we assumed $U_0'' \approx |U_b''|$.

We thus estimate E_b as a function of $\langle S\rangle_{t_R}$: $E_b/k_BT = E_0/k_BT + f\langle S\rangle_{t_R}$, with $E_0/k_BT = 12.8$, $f = -0.21$ for large-, and $E_0/k_BT = 11.0$, $f = -0.26$ for small particles [Fig. 5(a)]. These E_b' s are in the same range as simulations [18,49,52] when supercooled behavior starts to emerge. The mean barrier height for large particles is $1.8k_BT$ more than small particles; larger particles are more arrested in the bidisperse system [53]. Combining $P(\langle S\rangle_{t_R})$ and $E_b(\langle S\rangle_{t_R})$ results, we obtain the probability distribution $P(E_b)$ of activation energy barriers [Fig. 5(b)].

To conclude, we experimentally demonstrated that softness is effective in classifying particle-hopping frequency in thermal, supercooled colloidal liquids. Particles with the same softness had local structural environments similar enough to give rise to exponential relaxation with a single activation time. We further demonstrated that the measured

combination of exponential distributions produces the observed nonexponential relaxation behavior of the whole sample, and we estimated activation energy barriers and their distribution. These demonstrated capabilities in a thermal system represent first experimental steps towards exploration of thermal supercooled colloidal liquids and glasses, i.e., in a way that permits simultaneous access to key structural, dynamical, and thermodynamic information. Equilibrium and nonequilibrium studies under a range of interesting conditions, including varying density and fragility, during aging, and under shear should be possible.

We thank Kevin Aptowicz, Coline Bretz, Rob Carpick, Peter Collings, Doug Durian, Stefan Egelhaaf, Zahra Fakhraai, Matt Gratale, Piotr Habdas, Jürgen Horbach, Rob Riggleman, Ken Schweizer, and Daniel Sussman for helpful discussions. X. M., Z. S. D., T. S., and A. G. Y. gratefully acknowledge financial support from the National Science Foundation through DMR16-07378, MRSEC DMR-1720530 including its Optical Microscopy Shared Experimental Facility, and NASA NNX08AO0G. R. I., S. S. S., and A. J. L. gratefully acknowledge financial support from the U.S. Department of Energy, Office of Basic Energy Sciences, Division of Materials Sciences and Engineering through Award No. DE-FG02-05ER46199 and the Simons Foundation (Grant No. 327939 to A. J. L.).

X. M. and Z. S. D. contributed equally to this work.

*xiaom@seas.upenn.edu

[1] F. Spaepen and D. Turnbull, Metallic glasses, Annu. Rev. Phys. Chem. **35**, 241 (1984).
[2] W. Götze and L. Sjogren, Relaxation processes in supercooled liquids, Rep. Prog. Phys. **55**, 241 (1992).
[3] F. H. Stillinger, A topographic view of supercooled liquids and glass formation, Science **267**, 1935 (1995).
[4] J. C. Dyre, The glass transition and elastic models of glass-forming liquids, Rev. Mod. Phys. **78**, 953 (2006).
[5] G. Tarjus, in *Dynamical Heterogeneities in Glasses, Colloids, and Granular Media*, edited by L. Berthier, G. Biroli, J.-P. Bouchaud, L. Cipelletti, and W. van Saarloos (Oxford University Press, Oxford, 2011), Chap. 2.
[6] J. Gilman, Metallic glasses, Phys. Today **28**, No. 5, 46 (1975).
[7] L. Berthier and R. L. Jack, Structure and dynamics of glass formers: Predictability at large length scales, Phys. Rev. E **76**, 041509 (2007).
[8] C. P. Royall, S. R. Williams, T. Ohtsuka, and H. Tanaka, Direct observation of a local structural mechanism for dynamic arrest, Nat. Mater. **7**, 556 (2008).
[9] A. Widmer-Cooper, H. Perry, P. Harrowell, and D. R. Reichman, Irreversible reorganization in a supercooled liquid originates from localized soft modes, Nat. Phys. **4**, 711 (2008).
[10] M. L. Manning and A. J. Liu, Vibrational Modes Identify Soft Spots in a Sheared Disordered Packing, Phys. Rev. Lett. **107**, 108302 (2011).
[11] K. Chen, M. L. Manning, P. J. Yunker, W. G. Ellenbroek, Z. Zhang, A. J. Liu, and A. G. Yodh, Measurement of Correlations Between Low-Frequency Vibrational Modes and Particle Rearrangements in Quasi-Two-Dimensional Colloidal Glasses, Phys. Rev. Lett. **107**, 108301 (2011).
[12] A. Ghosh, V. Chikkadi, P. Schall, and D. Bonn, Connecting Structural Relaxation with the Low Frequency Modes in a Hard-Sphere Colloidal Glass, Phys. Rev. Lett. **107**, 188303 (2011).
[13] R. L. Jack, A. J. Dunleavy, and C. P. Royall, Information-Theoretic Measurements of Coupling Between Structure and Dynamics in Glass-Formers, Phys. Rev. Lett. **113**, 095703 (2014).
[14] L. Berthier and G. Biroli, Theoretical perspective on the glass transition and amorphous materials, Rev. Mod. Phys. **83**, 587 (2011).
[15] C. P. Royall and S. R. Williams, The role of local structure in dynamical arrest, Phys. Rep. **560**, 1 (2015).
[16] S. Gokhale, A. K. Sood, and R. Ganapathy, Deconstructing the glass transition through critical experiments on colloids, Adv. Phys. **65**, 363 (2016).
[17] E. D. Cubuk, S. S. Schoenholz, J. M. Rieser, B. D. Malone, J. Rottler, D. J. Durian, E. Kaxiras, and A. J. Liu, Identifying Structural Flow Defects in Disordered Solids Using Machine-Learning Methods, Phys. Rev. Lett. **114**, 108001 (2015).
[18] S. S. Schoenholz, E. D. Cubuk, D. M. Sussman, E. Kaxiras, and A. J. Liu, A structural approach to relaxation in glassy liquids, Nat. Phys. **12**, 469 (2016).
[19] S. S. Schoenholz, E. D. Cubuk, E. Kaxiras, and A. J. Liu, Relationship between local structure and relaxation in out-of-equilibrium glassy systems, Proc. Natl. Acad. Sci. U.S.A. **114**, 263 (2017).
[20] D. M. Sussman, S. S. Schoenholz, E. D. Cubuk, and A. J. Liu, Disconnecting structure and dynamics in glassy thin films, Proc. Natl. Acad. Sci. U.S.A. **114**, 10601 (2017).
[21] E. D. Cubuk, S. S. Schoenholz, E. Kaxiras, and A. J. Liu, Structural properties of defects in glassy liquids, J. Phys. Chem. B **120**, 6139 (2016).
[22] E. D. Cubuk *et al.*, Structure-property relationships from universal signatures of plasticity in disordered solids, Science **358**, 1033 (2017).
[23] T. A. Sharp, M. Merkel, M. L. Manning, and A. J. Liu, Statistical properties of 3D cell geometry from 2D slices, arXiv:1802.09131.
[24] K. Schmidt-Rohr and H. W. Spiess, Nature of Nonexponential Loss of Correlation above the Glass Transition Investigated by Multidimensional NMR, Phys. Rev. Lett. **66**, 3020 (1991).
[25] M. T. Cicerone and M. D. Ediger, Relaxation of spatially heterogeneous dynamic domains in supercooled orthoterphenyl, J. Chem. Phys. **103**, 5684 (1995).
[26] M. D. Ediger, Spatially heterogeneous dynamics in supercooled liquids, Annu. Rev. Phys. Chem. **51**, 99 (2000).
[27] A. Cavagna, Supercooled liquids for pedestrians, Phys. Rep. **476**, 51 (2009).
[28] W. Ostwald, Notiz über das elektrische Leitungsvermögen der Säuren, J. Prakt. Chem. **30**, 93 (1884).
[29] J. H. Van't Hoff, in *Etudes de Dynamiques Chimiques* (F. Muller and Co., Amsterdam, 1884), p. 114; Translated

by T. Ewan as *Studies in Chemical Dynamics* (Williams & Norgate, London, 1896).
[30] S. Arrhenius, Über die Reaktionsgeschwindigkeit bei der Inversion von Rohrzucker durch Säuren, Z. Phys. Chem. **4**, 226 (1889).
[31] H. A. Kramers, Brownian motion in a field of force and the diffusion model of chemical reactions, Physica (Utrecht) **7**, 284 (1940).
[32] See Supplemental Material at http://link.aps.org/supplemental/10.1103/PhysRevLett.122.028001 for details.
[33] T. Still, K. Chen, A. M. Alsayed, K. B. Aptowicz, and A. G. Yodh, Synthesis of micrometer-size poly(N-isopropylacrylamide) microgel particles with homogeneous crosslinker density and diameter control, J. Colloid Interface Sci. **405**, 96 (2013).
[34] J. C. Crocker and D. G. Grier, Methods of digital video microscopy for colloidal studies, J. Colloid Interface Sci. **179**, 298 (1996).
[35] D. B. Allan, T. A. Caswell, and N. C. Keim, *Trackpy v0.2 (Version v0.2.0)* (Zenodo, Geneva, 2014).
[36] R. Candelier, A. Widmer-Cooper, J. K. Kummerfeld, O. Dauchot, G. Biroli, P. Harrowell, and D. R. Reichman, Spatiotemporal Hierarchy of Relaxation Events, Dynamical Heterogeneities, and Structural Reorganization in a Supercooled Liquid, Phys. Rev. Lett. **105**, 135702 (2010).
[37] A. Smessaert and J. Rottler, Distribution of local relaxation events in an aging three-dimensional glass: Spatiotemporal correlation and dynamical heterogeneity, Phys. Rev. E **88**, 022314 (2013).
[38] J. Mattsson, H. M. Wyss, A. Fernandez-Nieves, K. Miyazaki, Z. B. Hu, D. R. Reichman, and D. A. Weitz, Soft colloids make strong glasses, Nature (London) **462**, 83 (2009).
[39] R. Pastore, A. Coniglio, and M. P. Ciamarra, Dynamic phase coexistence in glass forming liquids, Sci. Rep. **5**, 11770 (2015).
[40] R. Pastore, A. Coniglio, A. de Candia, A. Fierro, and M. P. Ciamarra, Cage-jump motion reveals universal dynamics and non-universal structural features in glass forming liquids, J. Stat. Mech. (2016) 054050.
[41] R. Pastore, M. P. Ciamarra, G. Pesce, and A. Sasso, Connecting short and long time dynamics in hardsphere-like colloidal glasses, Soft Matter **11**, 622 (2015).
[42] B. E. Boser, I. Guyon, and V. Vapnik, A training algorithm for optimal margin classifiers, in *Proceedings of the Fifth Annual Workshop on Computational Learning Theory* (ACM Press, New York, 1992), pp. 144–152.
[43] F. Pedregosa *et al.*, Scikit-learn: Machine Learning in Python, J. Mach. Learn. Res. **12**, 2825 (2011).
[44] G. C. Cawley and N. L. C. Talbot, Over-fitting in model selection and subsequent selection bias in performance evaluation, J. Mach. Learn. Res. **11**, 2079 (2010).
[45] R. Pastore, G. Pesce, A. Sasso, and M. P. Ciamarra, Cage size and jump precursors in glass-forming liquids: Experiment and simulations, J. Phys. Chem. Lett. **8**, 1562 (2017).
[46] P. Hänggi, P. Talkner, and M. Borkovec, Reaction-rate theory: fifty years after Kramers, Rev. Mod. Phys. **62**, 251 (1990).
[47] K. S. Schweizer and E. J. Saltzman, Entropic barriers, activated hopping, and the glass transition in colloidal suspensions, J. Chem. Phys. **119**, 1181 (2003).
[48] E. J. Saltzman and K. S. Schweizer, Activated hopping and dynamical fluctuation effects in hard sphere suspensions and fluids, J. Chem. Phys. **125**, 044509 (2006).
[49] X. Du and E. R. Weeks, Energy barriers, entropy barriers, and non-Arrhenius behavior in a minimal glassy model, Phys. Rev. E **93**, 062613 (2016).
[50] X.-G. Ma, P.-Y. Lai, and P. Tong, Colloidal diffusion over a periodic energy landscape, Soft Matter **9**, 8826 (2013).
[51] Y. Su, X. G. MA, P. Y. Lai, and P. Tong, Colloidal diffusion over a quenched two-dimensional random potential, Soft Matter **13**, 4773 (2017).
[52] A. Heuer, Exploring the potential energy landscape of glass-forming systems: From inherent structures via metabasins to macroscopic transport, J. Phys. Condens. Matter **20**, 373101 (2008).
[53] R. Kurita and E. R. Weeks, Glass transition of two-dimensional binary soft-disk mixtures with large size ratios, Phys. Rev. E **82**, 041402 (2010).